Published in "Nature Structural & Molecular Biology 24(1): 15–22, 2017"
which should be cited to refer to this work.

Reciprocal regulation of carbon monoxide metabolism and the circadian clock

Roman Klemz[1], Silke Reischl[1], Thomas Wallach[1], Nicole Witte[2], Karsten Jürchott[1], Sabrina Klemz[1], Veronika Lang[1], Stephan Lorenzen[3], Miriam Knauer[2], Steffi Heidenreich[2], Min Xu[4], Jürgen A Ripperger[5], Michael Schupp[2], Ralf Stanewsky[4,6] & Achim Kramer[1]

Circadian clocks are cell-autonomous oscillators regulating daily rhythms in a wide range of physiological, metabolic and behavioral processes. Feedback of metabolic signals, such as redox state, NAD^+/NADH and AMP/ADP ratios, or heme, modulate circadian rhythms and thereby optimize energy utilization across the 24-h cycle. We show that rhythmic heme degradation, which generates the signaling molecule carbon monoxide (CO), is required for normal circadian rhythms as well as circadian metabolic outputs. CO suppresses circadian transcription by attenuating CLOCK–BMAL1 binding to target promoters. Pharmacological inhibition or genetic depletion of CO-producing heme oxygenases abrogates normal daily cycles in mammalian cells and *Drosophila*. In mouse hepatocytes, suppression of CO production leads to a global upregulation of CLOCK–BMAL1-dependent circadian gene expression and dysregulated glucose metabolism. Together, our findings show that CO metabolism is an important link between the basic circadian-clock machinery, metabolism and behavior.

In animals, fundamental clock mechanisms are highly conserved and are based on autoregulatory feedback loops that generate molecular oscillations in the transcript levels of approximately 5–10% of genes in essentially all tissues. In mammals, the transcription-factor heterodimer CLOCK–BMAL1 (or NPAS2–BMAL1) activates the transcription of *Per1*, *Per2* and *Per3* (denoted *Period*) and *Cry1* and *Cry2* (denoted *Cryptochrome*) genes from E-box enhancer elements, whose protein products form complexes inhibiting CLOCK–BMAL1 transactivational activity after a delay of several hours. In additional feedback loops, CLOCK–BMAL1 also supports the rhythmic expression of *Rev-Erbα* and *Rev-Erbβ* (official symbols *Nr1d1 and Nr1d2*, respectively), which modulate the expression of *Bmal1* (official symbol *Arntl*), and D-site-binding protein (*Dbp*), which modulates the expression of *Per2* (ref. 1).

Although circadian-clock regulation of many metabolic processes is well established, there is increasing evidence that metabolic signals feed back to the circadian oscillator and consequently adjust metabolic pathways within individual cells[2]. Heme, an iron-containing porphyrin that serves as a prosthetic group in several hemoproteins, has also been described to be a ligand of REV-ERBα. Heme binding to REV-ERBα supports co-repressor recruitment and transcriptional repression[3–5], thereby coordinating circadian and metabolic pathways. In addition, heme binding to NPAS2 *in vitro* mediates the CO-sensitive DNA binding of NPAS2–BMAL1 (ref. 6).

Heme synthesis is governed by the rate-limiting enzyme aminolevulinate synthase 1 (*Alas1*), which is negatively regulated by glucose and heme concentrations[7]. In addition, *Alas1* transcription is circadian, through transcriptional regulation by NPAS2–BMAL1 (ref. 8). Heme catabolism is mediated by heme oxygenases 1 and 2 (*Ho-1* and *Ho-2*; official symbols *Hmox1* and *Hmox2*, respectively), which generate biliverdin (and subsequently bilirubin), iron and carbon monoxide at the expense of nicotinamide adenine dinucleotide phosphate (NADPH)[9]. Although heme can regulate the transcription of *Period* genes[8], and circadian heme proteins may sense the redox state and potentially diatomic gases such as oxygen, nitric oxide and CO, the relevance of heme catabolism to circadian transcription and dynamics is unknown.

RESULTS

Inhibition of heme degradation alters circadian dynamics

To test whether cellular heme levels are critical for circadian dynamics, we treated human U2-OS reporter cells expressing firefly luciferase from a *Bmal1* promoter fragment with various concentrations of either hemin (iron protoporphyrin) or cobalt protoporphyrin, a specific inhibitor of the heme-degrading heme oxygenases[10,11]. Both compounds probably lead to increased intracellular heme levels either by providing additional heme or by inhibiting heme degradation. Whereas hemin treatment had no effect on the circadian period, the inhibition of heme degradation by cobalt protoporphyrin resulted in an inhibitor-dose-dependent lengthening of the circadian period of up to 1.5 h (**Fig. 1**). Thus, in this assay, heme-degradation products rather than the heme level itself were critical for circadian dynamics.

[1]Laboratory of Chronobiology, Charité Universitätsmedizin Berlin, Berlin, Germany. [2]Institute of Pharmacology, Center for Cardiovascular Research CCR, Charité Universitätsmedizin Berlin, Berlin, Germany. [3]Bernhard-Nocht-Institut, Hamburg, Germany. [4]Department of Cell and Developmental Biology, University College London, London, UK. [5]Division of Biochemistry, Department of Biology, University of Fribourg, Fribourg, Switzerland. [6]Present address: Westfälische Wilhelms-Universität Münster, Münster, Germany. Correspondence should be addressed to A.K. (achim.kramer@charite.de).

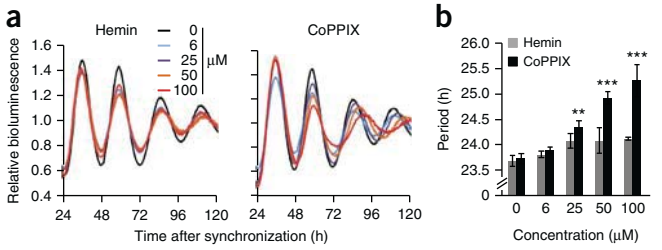

Figure 1 Inhibition of heme degradation alters circadian dynamics in human cells. (**a**) Circadian oscillation dynamics of dexamethasone-synchronized human osteosarcoma cells (U2-OS) bearing a *Bmal1* promoter–luciferase reporter construct treated with the indicated concentrations of hemin or the heme oxygenase inhibitor cobalt protoporphyrin (CoPPIX). Shown are detrended average time series of six parallel treatments. (**b**) Circadian periods of time series shown in **a** (mean ± s.d.; $n = 6$ independent cell cultures). Two-way ANOVA with Bonferroni post test revealed a significant difference between hemin and CoPPIX effects ($P < 0.0001$) and concentration ($P < 0.0001$). Three independent experiments yielded similar results. $^{**}P < 0.01$; $^{***}P < 0.001$.

Heme degradation is regulated by the circadian clock

The intricate connection between the circadian and metabolic systems manifests itself in that metabolic feedbacks into the circadian oscillator often have a circadian component. To test whether heme degradation is regulated by the circadian clock, we analyzed transcript and activity levels of *Ho-1*, the major heme-degrading enzyme in peripheral tissues[9]. In regular 6-h intervals over the course of two consecutive days, we harvested livers from mice kept in constant darkness and determined *Ho-1* transcript levels by quantitative RT–PCR. *Ho-1* expression showed a circadian rhythm with a peak at circadian time (CT) 12–15 and an approximately three-fold peak-to-trough ratio (**Fig. 2a**), results consistent with findings in peritoneal macrophages (**Supplementary Fig. 1a**) and with the diurnal variation observed by Xu and colleagues in liver tissue[12].

Transcription of *Ho-1* is induced by heme via stress-response enhancer elements (StREs) in its promoter[13]. To test whether rhythmic *Ho-1* expression is regulated by potentially rhythmic heme levels, we applied constant high concentrations of heme or cobalt protoporphyrin to synchronized primary hepatocytes. Whereas we observed the expected increase in *Ho-1* transcription (and HO-1 activity, in the case of heme treatment), circadian oscillations persisted (**Fig. 2b**) but were absent in hepatocytes from *Bmal1*$^{-/-}$ mice (**Supplementary Fig. 1b**). This finding indicates that rhythmic *Ho-1* regulation is different from rhythmic StRE activation and depends on the canonical circadian oscillator. Importantly, the activity of heme oxygenase was also rhythmic in the liver in both basal and heme-induced conditions (**Fig. 2c**), thus indicating that heme is rhythmically degraded. Interestingly, expression of *Alas1*, which encodes the rate-limiting enzyme in the heme biosynthesis pathway, is also rhythmic with a similar phase[8] to that of *Ho-1*, thus suggesting a potential mechanism for intracellular heme homeostasis.

To investigate whether *Ho-1* is a direct output gene of the circadian clock, we searched for clock-controlled enhancer elements within the *Ho-1* promoter and identified a highly conserved E box close to the transcription start site (**Supplementary Fig. 1c**). A 1,000-bp fragment of the *Ho-1* promoter was activated by CLOCK–BMAL1 in HEK293 cells and repressed by CRY1, but this regulation was abolished by E-box mutation (**Fig. 2d**). In addition, chromatin immunoprecipitation (ChIP) experiments on liver nuclei revealed that the *Ho-1* E box was occupied by endogenous BMAL1 in a manner dependent on the time of day (**Fig. 2e**). Moreover, transcript levels of *Ho-1* were deceased in the hepatocytes of *Bmal1*$^{-/-}$ mice (**Supplementary Fig. 1d**). Together, these results support the role of *Ho-1* as a direct target gene of CLOCK–BMAL1 *in vivo*.

The heme-degradation product CO modulates circadian transcription

Rhythmic heme degradation mediated by HO-1 leads to rhythmic accumulation of heme-degradation products, i.e., biliverdin, iron and CO. *In vitro*, CO inhibits binding of NPAS2–BMAL1 to DNA[6]. If such an inhibitory effect also occurs *in vivo*, transcription of NPAS2–BMAL1-target genes should increase when endogenous CO levels are decreased. Because heme oxygenase activity is the primary source of endogenous CO, and *Ho-1* is the dominant paralog in the periphery[13], we measured circadian transcript levels of CLOCK(NPAS2)–BMAL1-target genes in primary fibroblasts from *Ho-1*-knockout mice[14]. Indeed, transcript levels of clock genes containing functional promoter E boxes, such as *Dbp*, *Rev-Erbα* and *Per2*, were substantially upregulated, whereas transcription of *Bmal1* was downregulated during periods in which levels of the repressor REV-ERBα was high (**Fig. 3a**). The extent of this upregulation (for example, for *Dpb* transcript levels) was somewhat variable, ranging from 1.5-fold up to six-fold (**Supplementary Fig. 2**). It is likely that the effect of *Ho-1* depletion on E-box-controlled mRNA levels was transcriptional rather than post-transcriptional, because precursor (pre)-mRNA levels of *Dbp* and *Rev-Erbα* were similarly upregulated in *Ho-1*-knockout cells (**Supplementary Fig. 3a**). Thus, decreasing CO levels by downregulating heme oxygenase activity has a major effect on circadian transcription.

If the upregulation of E-box-containing circadian transcripts in *Ho-1*-knockout animals were due a decrease in endogenous CO levels, exogenous application of CO should, at least in part, reverse this transcriptional effect. Continuous application of 6% gaseous CO (compared with 6% nitrogen as a control for any hypoxia-induced effects) to primary fibroblasts from wild-type mice led to a slight decrease in expression of the E-box-controlled transcripts *Dbp* and *Rev-Erbα*, but not *Bmal1* (**Fig. 3b**). Similarly, acute CO application through use of CO-releasing molecules (CORMs) had only subtle effects on *Dbp* transcription in wild-type fibroblasts (discussion of the CO concentration in **Supplementary Note 1**). In contrast, acute or continuous CO treatment of *Ho-1*$^{-/-}$ primary fibroblasts substantially, yet not always completely, rescued high *Dbp* transcript levels in *Ho-1*-knockout fibroblasts (**Fig. 3c** and **Supplementary Fig. 2**). Importantly, this CO-mediated rescue was also present at the pre-mRNA level, a result consistent with the hypothesis that CO modulates transcription (**Supplementary Fig. 3b**).

CO suppresses transactivation and target-gene binding of CLOCK–BMAL1

To test whether CO-mediated transcriptional inhibition of genes containing functional E boxes correlates with CO inhibition of CLOCK(NPAS2)–BMAL1, we measured the transactivation activity of CLOCK–BMAL1 from an E-box-driven luciferase reporter in HEK293 cells treated with either CORMs or inactive controls (iCORMs). We found a CO-dose-dependent decrease in CLOCK–BMAL1-mediated transcription (**Fig. 4a**), thus indicating that CO directly regulates circadian transcriptional activity. This inhibitory effect is probably due to CO interfering with CLOCK(NPAS2)–BMAL1 binding to DNA, because ChIP experiments revealed that CO treatment decreased BMAL1 binding to the *Rev-Erbα* promoter in synchronized U2-OS cells at times when BMAL1 is transcriptionally active (**Fig. 4b**), although overall BMAL1 levels remained unchanged (**Supplementary Fig. 3c**).

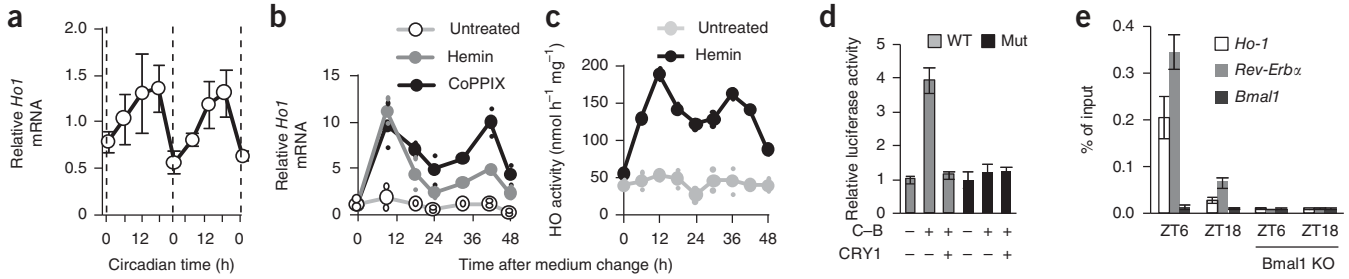

Figure 2 Heme degradation is regulated by the circadian clock. (**a**) Heme oxygenase 1 (*Ho-1*) transcript levels (normalized to *Hprt* and relative to mean levels) from mouse liver over 2 d in constant darkness (mean ± s.e.m.; $n = 4$ livers). (**b**) HO activity rhythms in untreated and hemin (30 μM)-stimulated primary hepatocytes. Shown are mean levels (large symbols) of two independent hepatocyte samples (small symbols). (**c**) *Ho-1* transcript rhythms (relative to *Hprt*) in primary hepatocytes treated with hemin or cobalt protoporphyrin (30 μM each). Data are normalized to mean levels of untreated control cells. Shown are mean levels (large symbols) of two independent hepatocyte samples (small symbols). (**d**) CLOCK–BMAL1 (C–B)-mediated transactivation and repression by CRY1 in HEK293 cells from a *Ho-1* promoter luciferase reporter with (mut) or without (WT) a mutated E box (mean ± s.e.m.; $n = 4$ independent cell cultures). (**e**) ChIP analysis of BMAL1 at the *Ho-1*, *Rev-Erbα* and *Bmal1* genes at zeitgeber time (ZT) ZT6 and ZT18 from wild-type or *Bmal1*$^{-/-}$ (*Bmal1* KO) liver chromatin (mean ± s.d.; $n = 6$ independent precipitations from liver samples from three mice per ZT and genotype). One-way ANOVA with a Bonferroni post test comparing all the different conditions indicated that the wild-type ZT6 data for the presence of BMAL1 at *Rev-Erbα* or *Ho-1* were highly significantly different from all other data for the same gene, and there were no such significant changes observed for the negative control, *Bmal1*.

Heme oxygenase–derived CO is essential for normal circadian dynamics in mammalian cells

The lengthening of the circadian period after pharmacological inhibition of heme oxygenases (**Fig. 1a**) suggested that heme oxygenase activity is an integral part of circadian-rhythm generation. To genetically test this phenomenon, we lentivirally transduced *Ho-1*$^{-/-}$ primary fibroblasts with a *Bmal1*-luciferase reporter construct and measured circadian-rhythm dynamics, but we were unable to detect a change in circadian period when this heme oxygenase was individually depleted (**Supplementary Fig. 4a**). We therefore further decreased heme oxygenase activity (**Supplementary Fig. 4b**), and thus probably endogenous CO levels, by RNA interference (RNAi)-mediated knockdown of the second active heme oxygenase paralog, *Ho-2* (ref. 15), in *Ho-1*$^{-/-}$ primary fibroblasts (genotype denoted *Ho-1*$^{-/-}$; *Ho-2*^{KD}). Circadian rhythms in these *Ho-1*$^{-/-}$; *Ho-2*^{KD} fibroblasts showed a substantial lengthening of the period by up to 2 h (**Fig. 5a** and **Supplementary Fig. 5a**), probably as a result of effects on circadian transcription, given that upregulation of the transcript

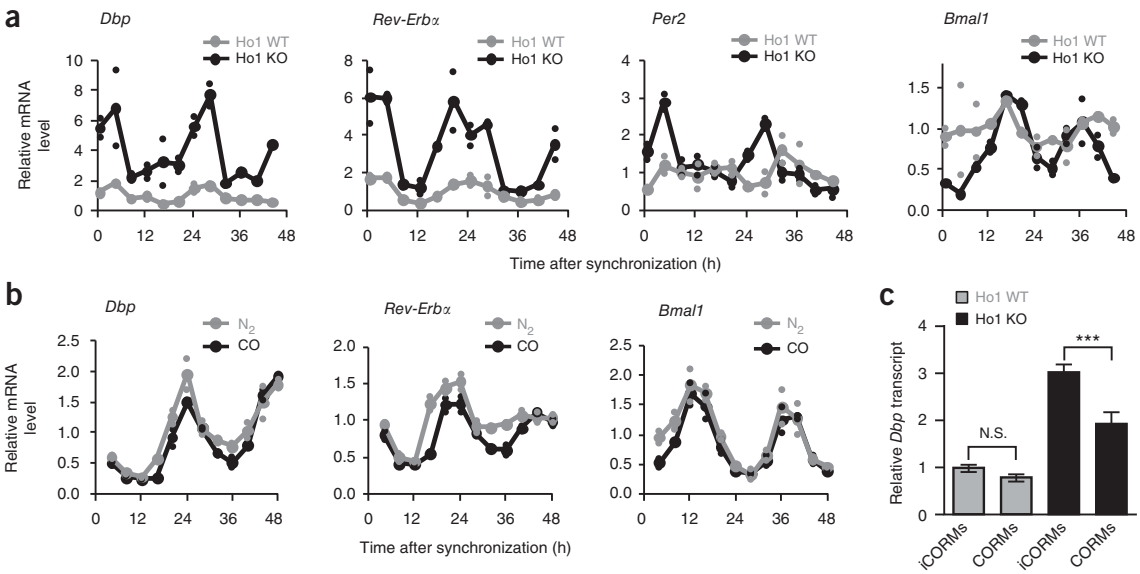

Figure 3 The heme-degradation product CO modulates circadian transcription. (**a**) Transcript rhythms of *Bmal1*, *Per2*, *Rev-Erbα* and *Dbp* in dexamethasone-synchronized primary fibroblasts from *Ho-1*$^{-/-}$ mice (Ho1 KO) or wild-type littermates (Ho1 WT). Data are normalized to *Hprt* expression and are presented relative to mean expression in wild-type cells. Shown are mean levels (large symbols) of two independent fibroblast samples from one mouse per genotype (small symbols). The amplitudes of sine fits (peak-to-trough ratios) for Ho1 WT versus Ho1 KO are 3.1 versus 2.9 for *Dbp*; 4.6 versus 6.1 for *Rev-Erbα*; 1.5 versus 3.2 for *Per2*; and 1.6 versus 3.4 for *Bmal1*. (**b**) Transcript rhythms of *Dbp*, *Rev-Erbα* and *Bmal1* in dexamethasone-synchronized primary fibroblasts from wild-type mice continuously treated with 6% CO or N_2. Normalization and presentation are as in **a**. (**c**) Transcript levels of *Dbp* in embryonic fibroblasts from *Ho-1*$^{-/-}$ mice (or wild-type littermates 24 h after dexamethasone synchronization, which were treated for 1 h with 100 μM CO-releasing molecules (CORMs) or inactive control molecules (iCORMs) before harvesting. Data are normalized to *Gapdh* expression and are presented relative to mean expression in wild-type cells treated with iCORMs. Data are shown as mean ± s.d. of three independent samples from one mouse per genotype. Two-way ANOVA with Bonferroni post test revealed a significant difference between genotypes ($P < 0.0001$) and drugs ($P < 0.0001$). ***$P < 0.001$; N.S., not significant. Similar experiments with samples from different mice are shown in **Supplementary Figure 2**.

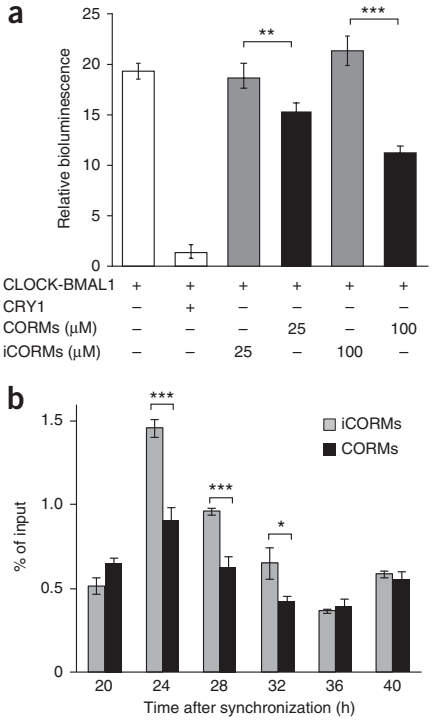

Figure 4 Carbon monoxide suppresses transactivation and target-gene binding of CLOCK–BMAL1. (**a**) CLOCK–BMAL1-mediated transactivation from an E-box-containing artificial promoter in HEK293 cells treated with CO-releasing molecules (CORMs) or inactive control molecules (iCORMs). Data are shown as mean ± s.d.; $n = 3$ independently transfected cell cultures. Two-way ANOVA with Bonferroni post test revealed a significant difference between iCORM and CORM treatments ($P < 0.0001$). ***$P < 0.001$; **$P < 0.01$. (**b**) ChIP analysis of BMAL1 bound to the *Rev-Erbα* gene in synchronized U2-OS cells treated with 100 μM CORMs or control iCORMs (mean ± s.e.m. of four pairwise comparisons). Two-way ANOVA with Bonferroni post test revealed a significant difference between genotype ($P < 0.0001$) and time ($P < 0.0001$). ***$P < 0.001$; *$P < 0.05$.

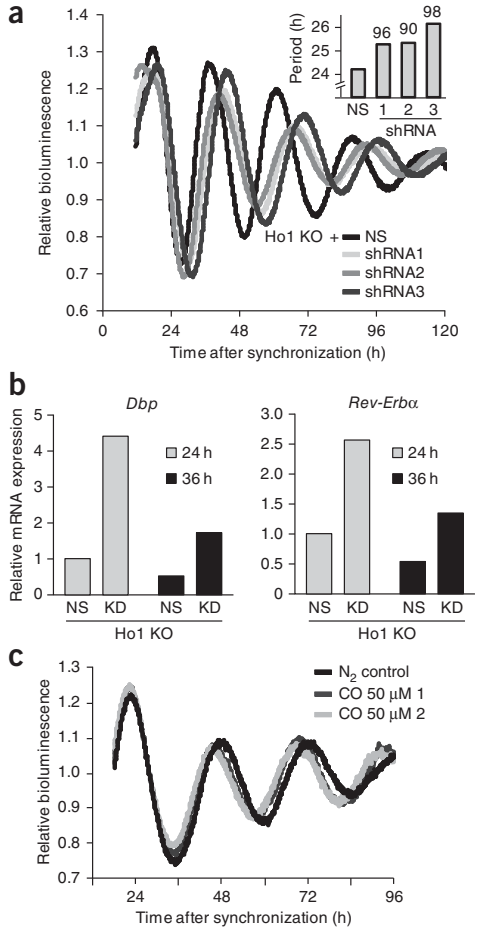

Figure 5 Heme oxygenases are essential for normal circadian dynamics in mammalian cells. (**a**) Circadian oscillation dynamics of synchronized primary fibroblasts from *Ho-1*$^{-/-}$ mice lentivirally transduced with (i) short hairpin RNA (shRNA) constructs targeting *Ho-2* or a nonsilencing (NS) control and (ii) a *Bmal1* promoter–luciferase reporter construct. Shown are representative examples of detrended time series (raw data in **Supplementary Fig. 5a**) and period quantification (inset; numbers above bars show percentage *Ho-2* mRNA knockdown). (**b**) Transcript levels of *Dbp* and *Rev-Erbα* 24 h and 36 h after dexamethasone synchronization of primary fibroblasts from *Ho-1*$^{-/-}$ mice transduced with an shRNA construct targeting *Ho-2* (KD) or a nonsilencing (NS) control. (**c**) Circadian dynamics of *Ho-1*$^{-/-}$; *Ho-2*^{KD} cells as in **a**, continuously treated with 6% CO or N_2. Shown are two representative examples of detrended time-series (raw data in **Supplementary Fig. 5b**).

levels of the E-box-controlled genes *Dbp* and *Rev-Erbα* was enhanced in the *Ho-1*$^{-/-}$; *Ho-2*^{KD} fibroblasts (**Fig. 5b**).

If depletion of endogenous CO in *Ho-1*$^{-/-}$; *Ho-2*^{KD} cells also contributes to the altered circadian dynamics, application of exogenous CO should be able to, at least in part, revert the period lengthening in *Ho-1*$^{-/-}$; *Ho-2*^{KD} cells. Indeed, continuous application of 6% CO, but not N_2, led to a reshortening of the circadian period in *Ho-1*$^{-/-}$; *Ho-2*^{KD} fibroblasts (**Fig. 5c** and **Supplementary Fig. 5b**) but had no effect on the circadian period in wild-type cells (**Supplementary Fig. 5c**), thus indicating that endogenous CO levels are essential for normal circadian-rhythm generation.

Heme oxygenase depletion globally alters clock-controlled transcription in hepatocytes

The strong effect of heme oxygenase depletion on circadian transcription and dynamics suggests a substantial effect on clock-controlled transcriptional output. To investigate this possibility globally, we performed microarray-based genome-wide transcriptional profiling of primary hepatocytes from wild-type or *Ho-1*$^{-/-}$ mice with or without additional knockdown of *Ho-2*. As expected from results in primary fibroblasts (**Fig. 3a**), circadian transcript levels of the clock-controlled genes *Dbp* and *Rev-Erbα* were upregulated in *Ho-1*$^{-/-}$ hepatocytes, even more so in *Ho-2*^{KD} hepatocytes and to the greatest extent in *Ho-1*$^{-/-}$; *Ho-2*^{KD} cells (**Fig. 6a**). We identified 2,335 genes that were differentially expressed among these genotypes and grouped them into six clusters according to their gene-expression patterns (**Fig. 6b** and **Supplementary Table 1**).

If heme oxygenase depletion acts globally on circadian transcriptional output, genes that are rhythmically expressed in the liver should be highly represented among differentially expressed genes[16]. This was indeed the case in cluster 1 ($P < 10^{-14}$) and to a lesser extent in cluster 2 ($P < 10^{-4}$) (**Fig. 6b**). Cluster 1 contained 473 genes whose transcript profiles were most similar to that of the E-box-containing clock-controlled gene *Dbp* (comparison with **Fig. 6a**). In addition, cluster 1 was highly enriched in genes reported to bind endogenous BMAL1 in ChIP experiments on liver chromatin ($P < 10^{-22}$ (ref. 17)), and genes with promoter E-box motifs (both E1 and E2 E boxes) were overrepresented only in cluster 1 (**Fig. 6c**). Although clusters 1 and 2 were

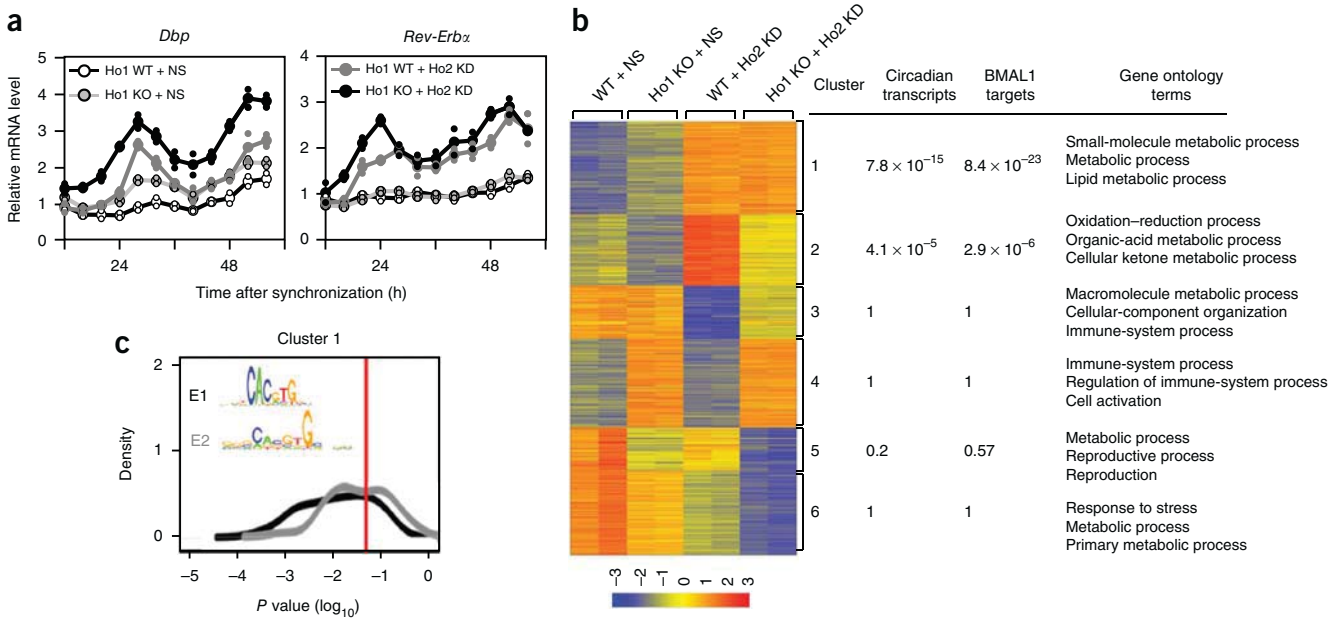

Figure 6 Heme oxygenase depletion globally alters clock-controlled transcription in hepatocytes. (**a**) Circadian transcription of *Dbp* and *Rev-Erbα* in synchronized primary hepatocytes of *Ho-1*$^{-/-}$ or wild-type littermate mice with or without additional *Ho-2* depletion by RNAi. Data are normalized to *Gapdh* expression and are presented relative to mean expression in wild-type cells transduced with the nonsilencing (NS) control. Shown are mean levels (large symbols) of two independent samples from two mice (small symbols). (**b**) Left, Heat diagram sorted in six clusters, showing changes in gene expression detected in a microarray experiment with hepatocytes, as described in **a**, 24 h after synchronization, the time of maximal CLOCK–BMAL1 binding to DNA ($n = 2$ mice per genotype). Increases (red) or decreases (blue) in transcript levels are shown. Middle, *P* values indicate significance for overrepresentation (Fisher's test) of genes with a circadian transcript in liver[16] or with BMAL1 binding in their promoters[17]. Right, Most significant nonredundant gene ontology terms for genes enriched in the clusters. (**c**) Bioinformatics analysis of cluster 1 genes for overrepresentation of E-box motifs in regions from −1,000 bp to +1,000 bp with respect to the transcription start site. Shown are *P*-value distributions of TRAP scores (Online Methods) for depicted E-box motifs compared with background gene sets.

also enriched in target genes of REV-ERBα and REV-ERBβ (ref. 18), we believe that it is unlikely that the upregulation of these targets in *Ho-1*- and *Ho-2*-depleted hepatocytes was due to CO directly regulating the activity of REV-ERBα and REV-ERBβ (discussion in **Supplementary Note 2**).

Heme oxygenase depletion alters glucose homeostasis

Gene ontology analysis revealed significant enrichment of genes involved in metabolic processes in cluster 1, whereas in the *Ho-1*-dominated cluster 4, the significant GO terms reflect known roles of *Ho-1* in cytoprotection and immune response[13,14] (**Fig. 6b**). Genes

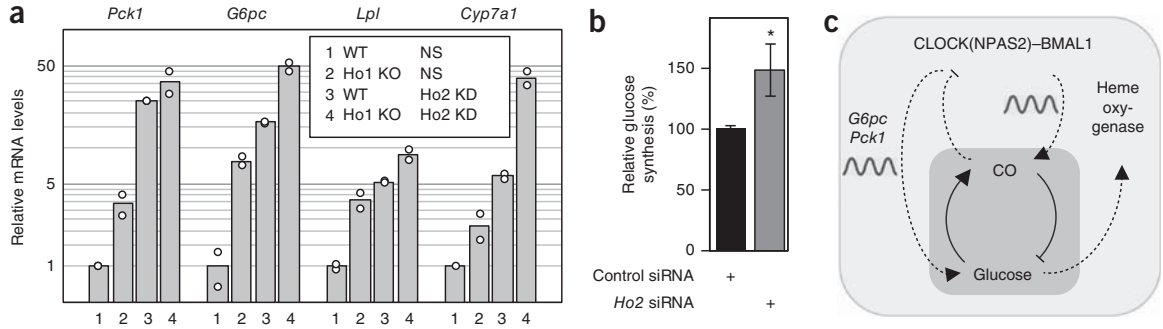

Figure 7 Interplay between carbon monoxide and glucose metabolism. (**a**) Transcript levels of *Pck1*, *G6pc*, *Lpl* and *Cyp7a1* in primary hepatocytes (24 h after dexamethasone synchronization) of *Ho-1*$^{-/-}$ or wild-type littermate mice with or without additional *Ho-2* depletion by RNAi. Data are normalized to *Gapdh* expression and are presented relative to mean expression in wild-type cells transduced with the nonsilencing (NS) control. Shown are mean levels (bars) of two independent samples from two mice (small symbols). (**b**) *Ho-2* depletion via siRNA transfection increases glucagon-induced glucose production in hepatocytes (normalized to total protein content; mean ± s.d.; $n = 3$ independent transfections of hepatocyte cultures from the same mouse; $^*P < 0.05$ by two-tailed *t* test). Two independent experiments yielded similar results. (**c**) Schematic model of the feedback interplay between endogenous CO and glucose homeostasis. The core of this model (dark gray) describes the activation of CO production by high glucose and oxidative-stress levels and the negative influence of CO on glucose production. The mechanisms by which these regulatory influences are exerted are depicted in the light-gray area of the scheme: endogenous CO is rhythmically produced by heme oxygenases, whose transcription is activated by CLOCK(NPAS2)–BMAL1 (among other factors) (**Fig. 2**). CO has a negative influence on CLOCK(NPAS2)–BMAL1-mediated transcriptional activity (**Fig. 3** and **Fig. 4**), thereby also inhibiting genes important for glucose production (**Fig. 7a**). High glucose levels, however, lead to the induction of *Ho-1* (ref. 46) and thereby support endogenous CO production.

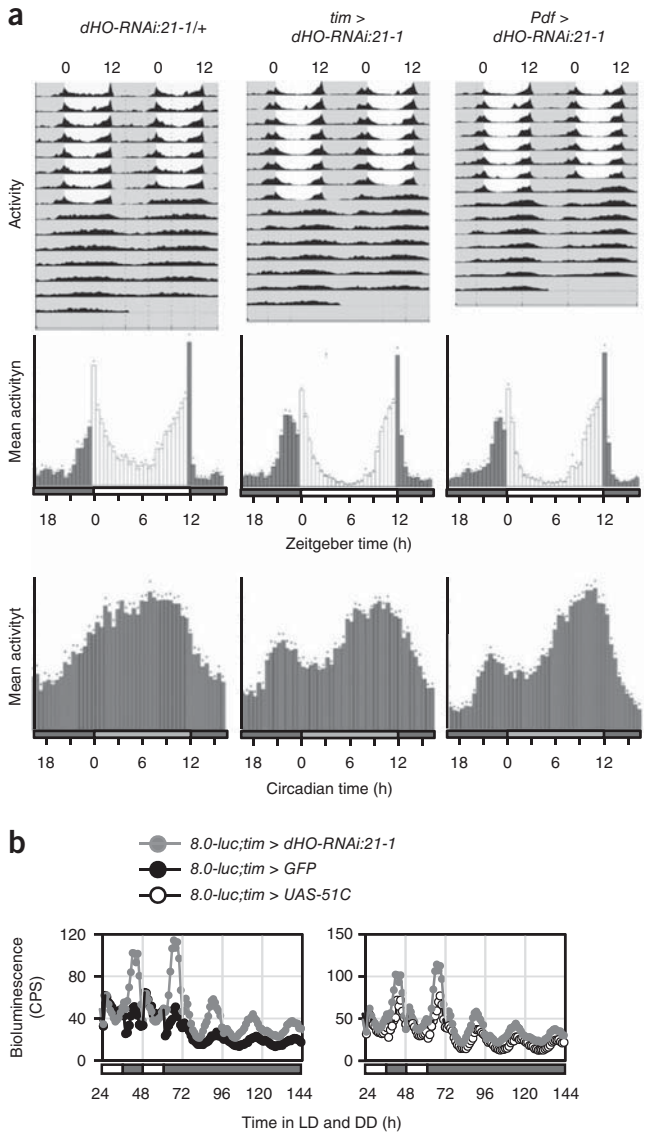

Figure 8 Heme oxygenase (*dHo*) is essential for normal daily activity patterns in *Drosophila*. (**a**) Average locomotor activity of *Drosophila* males in 12 h light–12 h dark conditions for 5–8 d, followed by 7 d in constant darkness (DD). Exact genotypes from left to right: *UAS-dHo-RNAi:21-1/+* (n = 15 flies); *timeless-gal4:62/UAS-dHo-RNAi:21-1* (n = 16 flies); *Pdf-gal4/UAS-dHo-RNAi:21-1* (n = 16 flies). Top, double-plotted actograms showing average activity during the entire experiment. Gray and white areas indicate dark and light periods, respectively. The morning peak in flies with decreased *dHo* expression persists in DD but disappears rapidly in the controls. Bottom, histograms showing average activity within in 30 min (bars); dark bars, 'lights off'; white bars, 'lights on', dots, s.e.m. The phase-advanced morning activity peak in flies with decreased *dHo* expression in clock cells. The same advance was observed in transgenic flies bearing a different *dHo-RNAi* construct (additional data and additional control genotypes in **Supplementary Fig. 7a**). (**b**) Real-time luciferase recordings of flies expressing a PERIOD-LUCIFERASE fusion protein in dorsal clock neurons encoded by the promoterless *8.0-luc* transgene[30]. Male flies were recorded in LD and DD, as indicated by the bars below the plots (white and black bars indicate lights on and lights off, respectively). Exact genotypes: gray circles, *8.0-luc/+;tim-gal4:67/UAS-dHo-RNAi:21-1* (n = 14 flies); black circles, 8.*0-luc/UAS-GFP;tim-gal4:67/+* (n = 10 flies); open circles, *8.0-luc/UAS-attP-51C;tim-gal4:67/+* (n = 10 flies). The peak levels were higher in LD and DD, and the amplitude of PER-LUC oscillations increased in *dHo-RNAi* flies. Similar results were obtained in two independent experiments and with the *dHo-RNAi:21-8* line (**Supplementary Fig. 7b**).

important in glucose and lipid metabolism, such as *Pck1*, *G6pc*, *Lpl* or *Cyp7a1*, were strongly upregulated in *Ho-1*$^{-/-}$; *Ho-2*^{KD} hepatocytes and to a lesser extent in *Ho-1*$^{-/-}$ and *Ho-2*^{KD} hepatocytes, as verified by quantitative RT–PCR (**Fig. 7a**). Again, heme oxygenase probably affects transcriptional rather than post-transcriptional processes, because the pre-mRNA levels of *Pck1*, *G6pc*, *Lpl* and *Cyp7a1* were similarly upregulated in heme oxygenase–depleted hepatocytes (**Supplementary Fig. 6**). Because *Pck1* and *G6pc* are important players in gluconeogenesis, we investigated the effect of acute small interfering RNA (siRNA)-mediated *Ho-2* depletion on glucagon-stimulated glucose production in primary hepatocytes. Consistently with the upregulation of these enzymes in *Ho-2*-depleted cells, we found a significant increase in glucagon-stimulated glucose production, thus suggesting that heme oxygenase activity is required for normal glucose homeostasis (**Fig. 7b**).

Heme oxygenase is essential for normal daily activity patterns in *Drosophila*

Because the expression of *Alas1* and heme oxygenase has also been reported to be circadian in *Drosophila melanogaster* heads[19,20], we investigated whether heme oxygenase (*dHo* (official symbol *Ho*), which is the only isoform of heme oxygenase in *Drosophila* and is essential for normal fly development[21]) is also required for normal rhythms in this species. To this end, we examined behavioral rhythms in flies in which *dHo* expression was knocked down in various cell types by two independent *UAS-dHo-RNAi* lines by using the binary Gal4–UAS system[22]. Under standard 12 h–12 h light–dark (LD) cycles, wild-type flies exhibit crepuscular behavior, with pronounced morning (M) and evening (E) activity peaks[23] (**Fig. 8a**). When released into constant dark conditions (DD), wild-type flies maintain their E peak, whereas the M peak weakens or disappears (**Fig. 8a**). Knockdown of *dHo* in all neurons (by using the pan-neuronal Gal4 driver *elav-gal4*) resulted in a substantially advanced M peak, whereas the E peak was unaffected (**Supplementary Fig. 7a**). Next, we downregulated *dHo* with the *timeless* (*tim*)*-gal4* driver, which is active in all clock neurons and peripheral clock cells throughout the body[24]. Also, using *Pdf-gal*, we directed *dHo* knockdown to the subset of the clock neurons important for regulating M activity[25–27]. In both cases, we observed a phase advance of the M peak, which, interestingly, was also maintained in the subsequent DD period, thus indicating that *dHo* knockdown in clock neurons somehow enhances M activity (**Fig. 8a** and **Supplementary Fig. 7a**). Clock cell-specific *dHo* knockdown had no effect on E activity or circadian period in DD, and *dHo* RNAi directed toward glia cells (by using the pan-glial driver *repo-gal4*) did not alter LD activity (**Fig. 8a**, **Supplementary Fig. 7a**, **Supplementary Table 2** and ref. 28). To test whether heme oxygenase depletion increases transcription from E-box-containing promoters, as observed in mammalian cells, we performed a real-time *in vivo* luciferase reporter assay for *Period* transcription in live flies[29]. Flies in which *dHo* was downregulated in all clock cells (*tim-gal4*) showed normal expression levels and temporal regulation of *Period*-promoter-driven luciferase expression under LD and DD conditions (**Supplementary Fig. 7b**). Similarly, clock cell-specific *dHO* RNAi had no effect on the expression of a *Period*-luciferase transgene reporter in central and peripheral clock cells[30] (**Supplementary Fig. 7b**). On the basis of the behavioral phenotype of *dHo* RNAi flies, we used a reporter that directs PERIOD expression in only a subset of the behavior-controlling clock neurons and that is not active in peripheral clock cells (*8.0-luc*[30]). Strikingly, and consistently with the observed strengthening of behavioral rhythms, *dHo* knockdown resulted in a substantial increase in *Period* expression from the luciferase reporter during the normal peak expression times

in LD and DD conditions, thus generating an increase in the overall amplitude of *Period* oscillations in LD (**Fig. 8b** and **Supplementary Fig. 7b**). Because the *8.0-luc* construct lacks the *Period* promoter sequences (including the E boxes), the observed increase in PERIOD expression was probably post-transcriptionally regulated. Together, these results indicate that in *Drosophila*, as in mammals, the circadian system requires heme oxygenase for temporal coordination of behavioral activity and circadian accumulation of clock proteins, but in the *Drosophila* system, in contrast to the mammalian system, this coordination is not accomplished via increased transcription.

DISCUSSION

Here, we show that endogenous CO production by heme oxygenase activity is required not only for circadian oscillator function but also for balanced clock-gene and clock-target-gene expression, thereby modulating glucose homeostasis in hepatocytes. Mechanistically, we favor the hypothesis that, in mammals, heme oxygenase–derived CO attenuates CLOCK(NPAS2)–BMAL1 DNA binding, probably via coordination by a heme molecule bound to NPAS2 (ref. 6) and probably also to CLOCK[31], and thereby modulates expression of CLOCK(NPAS2)–BMAL1-target genes. Although this scenario is not the only possible interpretation of our results (as described below), our preferred model is consistent with both past and present observations. (i) *In vitro*, micromolar concentrations of CO have been shown to impair DNA binding and BMAL-heterodimer formation of heme-bound NPAS2 but not apo-NPAS2 (ref. 6), and in the brain, these concentrations of CO are generated by heme oxygenases[32] (detailed discussion of CO concentration in **Supplementary Note 1**). (ii) Mutation of heme-coordinating residues within NPAS2 also impairs heterodimer formation with BMAL1, thus decreasing both specific DNA binding to canonical E boxes and NPAS2–BMAL1 transactivation activity, probably via conformational changes within the PAS-A domain of NPAS2 (ref. 33). (iii) Although much less is known about whether CLOCK is also able to bind heme and whether CO can modulate CLOCK activity, recent biophysical data have confirmed that the PAS-A domain of CLOCK binds heme *in vitro* with spectroscopic properties that are consistent with a sensor of diatomic gases[31]. (iv) We show here that depleting endogenous CO via heme oxygenase knockout leads to strong transcriptional upregulation of target genes of CLOCK(NPAS2)–BMAL1 in human and mouse hepatocytes. This observed modulation of circadian transcription is probably a direct effect of CO, because application of exogenous CO, but not N_2, suppresses CLOCK–BMAL1 transcriptional activation through E-box elements, attenuates transcription of endogenous CLOCK(NPAS2)–BMAL1 targets, partially rescues transcriptional upregulation in heme oxygenase knockouts and suppresses BMAL1 binding to target promoters.

Together, these observations provide compelling evidence of a role of endogenous CO in modulating the transcriptional stimulatory activity of CLOCK(NPAS2)–BMAL1. However, additional potential mechanisms underlying the influence of heme oxygenases on circadian transcription and dynamics are not eliminated, because heme degradation also produces biliverdin and iron in addition to CO. Moreover, heme degradation consumes NADPH, whose intracellular concentration modulates circadian dynamics and expression of CLOCK–BMAL1-target genes[34]. However, relevant to the present findings, we consider it unlikely that an increase in NADPH levels—as predicted to occur after heme oxygenase depletion—would generate long circadian periods and upregulation of CLOCK–BMAL1 targets, because such effects have previously been associated with decreased levels of NADPH[34].

It is also possible that CO indirectly influences circadian gene expression. The extent of CO's effect on CLOCK(NPAS2)–BMAL1 transcriptional activity is difficult to estimate. Although CO was originally considered to be a metabolic waste product, today most of the described anti-inflammatory, antiapoptotic, antiproliferative and cytoprotective roles of heme oxygenases are ascribed to CO[35]. Owing to the affinity of CO for metal ions, the few known CO sensors are heme-containing proteins including hemoglobin, myoglobin, soluble guanylyl cyclase (sGC), cytochrome *c* oxidase and the transcription factors Bach-1, Bach-2 and NPAS2. For example, heme oxygenase–derived CO can, like nitric oxide, activate sGC, thereby leading to increased levels of cGMP. Such a mechanism has been proposed to play a role in resetting the cholinergic clock in the suprachiasmatic nucleus[36], where heme oxygenase activity is circadian[37]. Moreover, increased cGMP levels can enhance AMP kinase (AMPK) activity[38], which in turn may act on the clock by promoting CRY-protein degradation[39]. Activation of AMPK in the liver also represses expression of gluconeogenesis enzymes such as *Pck1* and *G6pc*[40], results opposite from those observed in heme oxygenase–depleted hepatocytes. If the increases in *Pck1* and *G6pc* transcript levels in HO-depleted hepatocytes were due to decreased AMPK activity (perhaps mediated by increased oxidative stress[41]), transcript levels of genes involved in other anabolic pathways would also be expected to be elevated[42]. However, this was not the case: the expression of key genes involved in lipogenesis, such as sterol regulatory element–binding protein-1, carbohydrate response element–binding protein, acetyl CoA carboxylase, fatty acid synthase, stearoyl-CoA desaturase, and glycerol-3-phosphate acyltransferase, was essentially unaltered. Thus, modulation of AMPK activity is unlikely to be the cause of altered clock function and increased gluconeogenesis in heme oxygenase–depleted cells.

Our results further establish that heme oxygenase also functions in the *Drosophila* circadian clock. Downregulation of *dHo* leads to an advanced morning peak and to increased PERIOD levels and higher-amplitude oscillations in clock neurons, presumably via post-transcriptional regulation. The enhanced molecular oscillations may explain the robustness of the morning activity peak and the persistence of bimodal behavior under constant conditions. Typically, the morning activity peak weakens or disappears under constant conditions, whereas the evening peak is sustained, thus leading to unimodal behavior[43]. The enhanced molecular oscillations are reminiscent of the effects of the Pdf^{01} mutation on the same *8.0-luc* reporter used in the present study[44]. This reporter construct is expressed in a small subset of dorsal clock neurons, and enhanced *8.0-luc* oscillations in Pdf^{01} mutants are correlated with expression in additional dorsal clock neurons belonging to the evening oscillator, which show robust and synchronized PER oscillations in the absence of PDF[44]. Because we observed advanced morning activity after downregulation of *dHo* in only the PDF cells, it is possible that heme oxygenase may affect PDF or the communication between the PDF cells and the dorsal clock neurons expressing *8.0-luc*.

Interestingly, heme oxygenase activity has previously been linked to glucose homeostasis[15], and $Ho\text{-}2^{-/-}$ mice develop symptoms of type 2 diabetes, including hyperglycemia[45]. However, hepatocyte $Ho\text{-}1^{-/-}$ mice are insulin hypersensitive[46], and high glucose levels lead to *Ho-1* induction[47] as well as to increased CO exhalation[48]. Considering these results together with our present observation that heme oxygenase–depleted hepatocytes show increased gluconeogenesis, we suggest a feedback model that links CO production to the expression of genes important in glucose homeostasis (**Fig. 7c**). In our model, rhythmic heme oxygenase activity causes rhythmic CO production that in turn generates time-of-day-dependent repression of CLOCK(NPAS2)–BMAL1 transcriptional activation activity. CLOCK(NPAS2)–BMAL1-target genes supporting glucose production are thus inhibited by CO,

whereas high glucose levels lead to counter-regulation via heme oxygenase induction. Changes in redox state and heme levels not included in this feedback model are likely to have modulatory effects. It will be interesting to investigate whether CO, as a gaseous molecule, also contributes to intercellular circadian synchronization, thereby temporally coordinating metabolic signals within the organism.

METHODS

Methods, including statements of data availability and any associated accession codes and references, are available in the online version of the paper.

Note: Any Supplementary Information and Source Data files are available in the online version of the paper.

ACKNOWLEDGMENTS

We thank A. Grudziecki, B. Koller and U. Ungethüm for excellent technical support. We also thank M. Rauer and H. Herzel for bioinformatics help as well as A. Zenclusen (Otto von Guericke University Magdeburg), M. Brunner (Ruprecht-Karls-University Heidelberg), S. Taketani (Insect Biomedical Research Center, Kyoto Institute of Technology) and the NIG-Fly Stock Center (Genetic Strain Research Center, National Institute of Genetics Mishima) for materials. This work was supported by the BBSRC (grant BB/J018589/1 to R.S.) and the German Research foundation (Emmy Noether grant SCHU 2546/1-1 to M.S. and SFB 618/A4 and SFB 740/D2 to A.K.).

AUTHOR CONTRIBUTIONS

R.K., S.R., T.W., N.W., S.K., V.L., M.K., S.H., M.X. and J.A.R. performed experiments; K.J. performed bioinformatics analyses; S.L. provided the ChronoStar software; R.K., S.R., T.W., K.J., S.K., V.L., J.A.R., M.S., R.S. and A.K. designed experiments and analyzed data; R.S. and A.K. wrote the paper; and A.K. oversaw the project.

COMPETING FINANCIAL INTERESTS

The authors declare no competing financial interests.

1. Buhr, E.D. & Takahashi, J.S. Molecular components of the mammalian circadian clock. *Handb. Exp. Pharmacol.* **217**, 3–27 (2013).
2. Asher, G. & Schibler, U. Crosstalk between components of circadian and metabolic cycles in mammals. *Cell Metab.* **13**, 125–137 (2011).
3. Yin, L., Wu, N. & Lazar, M.A. Nuclear receptor Rev-erbalpha: a heme receptor that coordinates circadian rhythm and metabolism. *Nucl. Recept. Signal.* **8**, e001 (2010).
4. Yin, L. *et al.* Rev-erbalpha, a heme sensor that coordinates metabolic and circadian pathways. *Science* **318**, 1786–1789 (2007).
5. Raghuram, S. *et al.* Identification of heme as the ligand for the orphan nuclear receptors REV-ERBα and REV-ERBβ. *Nat. Struct. Mol. Biol.* **14**, 1207–1213 (2007).
6. Dioum, E.M. *et al.* NPAS2: a gas-responsive transcription factor. *Science* **298**, 2385–2387 (2002).
7. Oliveri, L.M., Davio, C., Batlle, A.M. & Gerez, E.N. ALAS1 gene expression is down-regulated by Akt-mediated phosphorylation and nuclear exclusion of FOXO1 by vanadate in diabetic mice. *Biochem. J.* **442**, 303–310 (2012).
8. Kaasik, K. & Lee, C.C. Reciprocal regulation of haem biosynthesis and the circadian clock in mammals. *Nature* **430**, 467–471 (2004).
9. Abraham, N.G. & Kappas, A. Pharmacological and clinical aspects of heme oxygenase. *Pharmacol. Rev.* **60**, 79–127 (2008).
10. Martasek, P. *et al.* Properties of human kidney heme oxygenase: inhibition by synthetic heme analogues and metalloporphyrins. *Biochem. Biophys. Res. Commun.* **157**, 480–487 (1988).
11. Sardana, M.K. & Kappas, A. Dual control mechanism for heme oxygenase: tin(IV)-protoporphyrin potently inhibits enzyme activity while markedly increasing content of enzyme protein in liver. *Proc. Natl. Acad. Sci. USA* **84**, 2464–2468 (1987).
12. Xu, Y.Q. *et al.* Diurnal variation of hepatic antioxidant gene expression in mice. *PLoS One* **7**, e44237 (2012).
13. Ryter, S.W., Alam, J. & Choi, A.M. Heme oxygenase-1/carbon monoxide: from basic science to therapeutic applications. *Physiol. Rev.* **86**, 583–650 (2006).
14. Yet, S.F. *et al.* Hypoxia induces severe right ventricular dilatation and infarction in heme oxygenase-1 null mice. *J. Clin. Invest.* **103**, R23–R29 (1999).
15. Satarug, S. & Moore, M.R. Emerging roles of cadmium and heme oxygenase in type-2 diabetes and cancer susceptibility. *Tohoku J. Exp. Med.* **228**, 267–288 (2012).
16. Hughes, M.E. *et al.* Harmonics of circadian gene transcription in mammals. *PLoS Genet.* **5**, e1000442 (2009).
17. Rey, G. *et al.* Genome-wide and phase-specific DNA-binding rhythms of BMAL1 control circadian output functions in mouse liver. *PLoS Biol.* **9**, e1000595 (2011).
18. Cho, H. *et al.* Regulation of circadian behaviour and metabolism by REV-ERB-α and REV-ERB-β. *Nature* **485**, 123–127 (2012).
19. Ceriani, M.F. *et al.* Genome-wide expression analysis in *Drosophila* reveals genes controlling circadian behavior. *J. Neurosci.* **22**, 9305–9319 (2002).
20. Ueda, H.R. *et al.* Genome-wide transcriptional orchestration of circadian rhythms in *Drosophila*. *J. Biol. Chem.* **277**, 14048–14052 (2002).
21. Cui, L. *et al.* Relevant expression of *Drosophila* heme oxygenase is necessary for the normal development of insect tissues. *Biochem. Biophys. Res. Commun.* **377**, 1156–1161 (2008).
22. Brand, A.H. & Perrimon, N. Targeted gene expression as a means of altering cell fates and generating dominant phenotypes. *Development* **118**, 401–415 (1993).
23. Hamblen-Coyle, M.J., Wheeler, D.A., Rutila, J.E., Rosbash, M. & Hall, J.C. Behavior of period-altered circadian rhythm mutants of *Drosophila* in light:dark cycles. *J. Insect Behav.* **5**, 417–446 (1992).
24. Kaneko, M. & Hall, J.C. Neuroanatomy of cells expressing clock genes in *Drosophila*: transgenic manipulation of the *period* and *timeless* genes to mark the perikarya of circadian pacemaker neurons and their projections. *J. Comp. Neurol.* **422**, 66–94 (2000).
25. Grima, B., Chélot, E., Xia, R. & Rouyer, F. Morning and evening peaks of activity rely on different clock neurons of the *Drosophila* brain. *Nature* **431**, 869–873 (2004).
26. Park, J.H. & Hall, J.C. Isolation and chronobiological analysis of a neuropeptide pigment-dispersing factor gene in *Drosophila melanogaster*. *J. Biol. Rhythms* **13**, 219–228 (1998).
27. Stoleru, D., Peng, Y., Agosto, J. & Rosbash, M. Coupled oscillators control morning and evening locomotor behaviour of *Drosophila*. *Nature* **431**, 862–868 (2004).
28. Mandilaras, K. & Missirlis, F. Genes for iron metabolism influence circadian rhythms in *Drosophila melanogaster*. *Metallomics* **4**, 928–936 (2012).
29. Stanewsky, R., Jamison, C.F., Plautz, J.D., Kay, S.A. & Hall, J.C. Multiple circadian-regulated elements contribute to cycling period gene expression in *Drosophila*. *EMBO J.* **16**, 5006–5018 (1997).
30. Veleri, S., Brandes, C., Helfrich-Förster, C., Hall, J.C. & Stanewsky, R. A self-sustaining, light-entrainable circadian oscillator in the *Drosophila* brain. *Curr. Biol.* **13**, 1758–1767 (2003).
31. Lukat-Rodgers, G.S., Correia, C., Botuyan, M.V., Mer, G. & Rodgers, K.R. Heme-based sensing by the mammalian circadian protein CLOCK. *Inorg. Chem.* **49**, 6349–6365 (2010).
32. Ingi, T., Cheng, J. & Ronnett, G.V. Carbon monoxide: an endogenous modulator of the nitric oxide-cyclic GMP signaling system. *Neuron* **16**, 835–842 (1996).
33. Ishida, M., Ueha, T. & Sagami, I. Effects of mutations in the heme domain on the transcriptional activity and DNA-binding activity of NPAS2. *Biochem. Biophys. Res. Commun.* **368**, 292–297 (2008).
34. Rey, G. *et al.* The pentose phosphate pathway regulates the circadian clock. *Cell Metab.* **24**, 462–473 (2016).
35. Kim, H.P., Ryter, S.W. & Choi, A.M. CO as a cellular signaling molecule. *Annu. Rev. Pharmacol. Toxicol.* **46**, 411–449 (2006).
36. Artinian, L.R., Ding, J.M. & Gillette, M.U. Carbon monoxide and nitric oxide: interacting messengers in muscarinic signaling to the brain's circadian clock. *Exp. Neurol.* **171**, 293–300 (2001).
37. Rubio, M.F., Agostino, P.V., Ferreyra, G.A. & Golombek, D.A. Circadian heme oxygenase activity in the hamster suprachiasmatic nuclei. *Neurosci. Lett.* **353**, 9–12 (2003).
38. Lira, V.A. *et al.* Nitric oxide increases GLUT4 expression and regulates AMPK signaling in skeletal muscle. *Am. J. Physiol. Endocrinol. Metab.* **293**, E1062–E1068 (2007).
39. Lamia, K.A. *et al.* AMPK regulates the circadian clock by cryptochrome phosphorylation and degradation. *Science* **326**, 437–440 (2009).
40. Cool, B. *et al.* Identification and characterization of a small molecule AMPK activator that treats key components of type 2 diabetes and the metabolic syndrome. *Cell Metab.* **3**, 403–416 (2006).
41. Shao, D. *et al.* A redox-dependent mechanism for regulation of AMPK activation by Thioredoxin1 during energy starvation. *Cell Metab.* **19**, 232–245 (2014).
42. Viollet, B. *et al.* AMPK: lessons from transgenic and knockout animals. *Front. Biosci. (Landmark Ed.)* **14**, 19–44 (2009).
43. Yoshii, T., Rieger, D. & Helfrich-Förster, C. Two clocks in the brain: an update of the morning and evening oscillator model in *Drosophila*. *Prog. Brain. Res.* **199**, 59–82 (2012).
44. Yoshii, T. *et al.* The neuropeptide pigment-dispersing factor adjusts period and phase of *Drosophila*'s clock. *J. Neurosci.* **29**, 2597–2610 (2009).
45. Sodhi, K. *et al.* Epoxyeicosatrienoic acid agonist rescues the metabolic syndrome phenotype of HO-2-null mice. *J. Pharmacol. Exp. Ther.* **331**, 906–916 (2009).
46. Jais, A. *et al.* Heme oxygenase-1 drives metaflammation and insulin resistance in mouse and man. *Cell* **158**, 25–40 (2014).
47. Chen, S., Khan, Z.A., Barbin, Y. & Chakrabarti, S. Pro-oxidant role of heme oxygenase in mediating glucose-induced endothelial cell damage. *Free Radic. Res.* **38**, 1301–1310 (2004).
48. Paredi, P., Biernacki, W., Invernizzi, G., Kharitonov, S.A. & Barnes, P.J. Exhaled carbon monoxide levels elevated in diabetes and correlated with glucose concentration in blood: a new test for monitoring the disease? *Chest* **116**, 1007–1011 (1999).

ONLINE METHODS

Mice. We used 6- to 8-week-old male C57Bl/6 mice for harvesting organs and fibroblast preparations. The animals were purchased from the Bundesinstitut für Risikobewertung (Berlin, Germany). *Ho-1*$^{-/-}$ mice (kind gift from A. Zenclussen) were raised with a normal diet and housed under and 12-h light–12-h dark conditions in the Animal Facility of Charité–Universitätsmedizin, Berlin, Germany. All mouse experiments were carried out in accordance with the German and European legal and ethical regulations and were approved by the Senatsverwaltung für Gesundheit und Soziales, Berlin, Germany.

Flies. As controls, wild-type *ATDD*[49] and *Df*1 *w (y w)* flies were used. *UAS-dHo-RNAi* line *21-1* (third-chromosome insertion), as previously described, decreases endogenous *dHo* expression by >50% (ref. 21). We obtained similar results with *UAS-dHo-RNAi* line *21-8*, bearing an independent X-chromosomal insertion of the same construct (**Supplementary Fig. 7a**). To exclude any off-target effects, two insertion lines from the NIG-Fly RNAi collection (http://www.shigen.nig.ac.jp/fly/nigfly/) (*UAS-dHo-RNAi* lines *R1* and *R3* inserted on chromosomes 3 and 2, respectively), bearing a *dHo-RNAi* construct targeting a different region of *dHo* RNA were tested (**Supplementary Fig. 7a**). As unrelated *UAS* controls, we used *UAS-GFP:T2* (ref. 24) and an insertion of an empty *pUASTattB* vector into the *attP* landing site at 51C[50]. *Pdf-gal4*, *tim-Gal4:62, 67, 27*, *repo-gal4* and *elav-gal4* have been described previously[24,51–53]. To record period-luciferase rhythms *8.0-luc:9, XLG-luc:1* (ref. 30) and *plo:3b-1I* (ref. 29) were crossed into the respective mutant and control backgrounds.

Activity monitoring of flies. Locomotor activity of individual male flies aged 3 to 4 d was recorded automatically with a *Drosophila* Activity Monitoring (DAM) system (Trikinetics) as previously described[54]. Flies were kept in glass tubes supplemented with 5% sucrose and 2% agar and kept under 12-h–12-h LD cycles at 25 °C for 5–8 d before being released into free-running conditions (DD and 25 °C). Calculation of the free-running period and plotting of daily average histograms and actograms was performed with the fly toolbox and MATLab software[55]. Autocorrelation was applied to determine the rhythmicity and free-running period in **Supplementary Table 1**, as previously described[54]. Flies with RS (rhythmicity statistics) >1.5 were considered to be rhythmic. Only rhythmic flies were included in the period calculation.

Isolation and culture of primary hepatocytes. Isolation of hepatocytes was performed essentially as previously described[56]. In brief, livers of anesthetized 6- to 12-week-old male WT C57BL/6J or *Ho-1*$^{-/-}$ mice were perfused with digestion buffer containing 5,000 U collagenase (Worthington Biochemical). After filtration and separation with a Percoll gradient (Biochrome), cells were seeded in gelatin (0.2% in PBS) or collagen-coated 12-well plates in Dulbecco's modified Eagle's medium (DMEM) containing 10% FBS (Invitrogen) and 1% penicillin/streptomycin (Gibco).

Isolation and culture of primary fibroblasts. 6- to 12-week-old male mice were sacrificed, and ear, lung or tail tissues were cut into very small pieces and incubated overnight in cell culture medium (DMEM supplemented with 20% FBS, penicillin/streptomycin and HEPES and amphotericin B (final concentration 2.5 µg/ml)) mixed with Liberase (Roche). The next day, cells were pelleted by centrifugation, seeded into a new dish and grown in medium containing 20% FBS and amphotericin B for 4 d. Then culture conditions were changed to normal cell culture medium containing 10% FBS and no amphotericin B. Cells were either frozen in liquid nitrogen or used directly in experiments.

Synchronization of circadian rhythms. Circadian rhythms were synchronized by treatment with 1 µM dexamethasone for 30–60 min.

RNA interference. *Experiments with shRNA.* Hairpin shRNAs in the pLKO.1 lentiviral vector designed by The RNAi Consortium (TRC) for mouse *Ho-2* were purchased from Thermo Scientific, OpenBiosystems. The following clone IDs were used: TRCN0000076353 (mature antisense, ATGTGAAGTAAAGTGCAGTGG), TRCN0000076356 (mature antisense, ATAGCTCCTTCTTAATGTTTC) and TRCN0000076357 (mature antisense, TGTAACGAGTATAAGCATGGG). As a nonsilencing control, a pLKO.1 vector containing scrambled shRNA (plasmid 1864, Addgene, hairpin sequence CCTAAGGTTAAGTCGCCCTCGCTC GAGCGAGGGCGACTTAACCTTAGG) was used. For lentivirus production, HEK293T cells (Thermo Scientific HCL4517, regularly tested for mycoplasma) were seeded in T25 flasks and transfected with 2.5 mg psPAX, 1.5 mg pMD2G and 3.5 mg of the respective lentiviral expression plasmid (RNAi constructs) with a CalPhos Mammalian Transfection Kit (BD Biosciences) according to the manufacturer's protocol. Virus-containing supernatants were filtered, and cells were transduced with 1 ml of virus filtrate plus 8 ng/ml protamine sulfate (Sigma). After 24 h, medium was exchanged to puromycin-containing (10 µg/ml) medium for selection.

Experiments with siRNA. After the attachment of hepatocytes to the cell culture plate, the medium was replaced with 500 µl of DMEM only, and cells were transfected with 1 nM of siRNA (Eurogentec) and 4 µl of Lipofectamine 2000 (Invitrogen) per well overnight. The next morning, the medium was replaced by DMEM containing 10% FBS and 1% penicillin/streptomycin.

Protoporphyrin preparation. For hemin (Fe^{3+}-protoporphyrin IX) and cobalt-protoporphyrin IX (Sigma-Aldrich), stock solutions of 1 mg/ml were prepared: 10 mg porphyrin was dissolved in 800 µl NaOH (0.2 M) and incubated for 30 min in darkness (RT). 8 ml PBS was added and the pH was adjusted to 7.4 with 150–200 µl of 1 M HCl.

Transfection and luciferase reporter assays. Transient transfections were carried out with Lipofectamine 2000 (Life Technologies) according to the manufacturer's protocol. HEK293 cells (human, ATCC CRL-1573, regularly tested for mycoplasma) were seeded in 24-well plates in antibiotic-free medium. Transfection was performed after cells had reached 80–90% confluence. The total amount of transfected DNA in each sample was 1.2 µg, composed of a firefly luciferase reporter construct (50 ng pGL3/mouse *Ho-1*_E-box_WT or 50 ng pGL3/mouse *Ho-1*_E-box_mut) and mouse *Clock* (300 ng), mouse *Bmal1* (300 ng) and mouse *Cry1* (30 ng), as indicated. For normalization, 2 ng of a *Renilla* luciferase vector pRL-SV40 was cotransfected. The total amount of DNA per well was adjusted to 1.2 µg by addition of empty pDEST26 vector. Cells were harvested 48 h after transfection in 200 µl passive lysis buffer (PLB) and frozen at −80 °C for 1 h. Cell lysates were homogenized by vortexing, and luciferase activity was measured with a Dual-Luciferase Reporter Assay System (Promega) according to the manufacturer's protocol, by using a 96-well-plate-reading luminometer (Orion II, Berthold Detection System). 5 µl of each cell extract was measured in duplicate by the addition of 25 µl LARII to measure firefly luciferase activity and then 25 µl Stop & Glo reagent to detect the *Renilla* luciferase activity. For data analysis, firefly luciferase activity was normalized to the corresponding *Renilla* luciferase activity.

Cloning and mutagenesis. The −1,000-bp region of the mouse *Ho-1* promoter was cloned into the luciferase reporter vector pGL3prom (Promega) by use of the KpnI and NheI restriction sites. The resulting luciferase reporter vector containing an E box (pGL3/mouse *Ho-1*_E-box_WT) was verified by DNA sequencing. Mutagenesis of the E box to an inactive form (CACGTG to TTTAGT; described in ref. 57) was performed by site-directed mutagenesis (QuikChange Site-Directed Mutagenesis Kit; Stratagene).

Live-cell and fly bioluminescence recording. U2-OS cells (human, ATCC HTB-96, regularly tested for mycoplasma) stably expressing firefly luciferase from a 0.9-kb *Bmal1* promoter fragment[58] were seeded into a white 96-well plate (20×10^4 cell/well). After 24 h, cells were synchronized with a single pulse of dexamethasone (1 µM) for 30 min. After being washed with PBS, cells were cultured in 150 µl phenol red–free DMEM containing 10% FBS, antibiotics (100 U/ml penicillin and 100 µg/ml streptomycin), and 250 µM D-luciferin (Biothema). Bioluminescence recordings were performed at 35–37 °C in a 96-well-plate-reading luminometer (TopCount, PerkinElmer). Primary fibroblasts were lentivirally transduced with reporter vector expressing firefly luciferase from a 0.9-kb *Bmal1* promoter fragment[58]. Bioluminescence rhythms were analyzed in light-tight boxes with a single photomultiplier tube (Hamamatsu Photonics). Raw data were detrended through division by the 24-h running average. Periods were estimated by fitting the cosine wave function with ChronoStar software, as described in ref. 58.

Luciferase expression of individual flies carrying the various period-luciferase transgenes were measured as described in ref. 30. Briefly, 2- to 3-d-old males were ether-anesthetized and loaded in a 96-well plate in which every other well

contained 100 µl of 5% sucrose, 1% agar and 15 mM luciferin (Biosynth). Flies were measured in a TopCount instrument (PerkinElmer) for 3 d in 12-h–12-h LD (25 °C) followed by DD for additional 3 d. Raw data were plotted with BRASS software (version 2.1.3) (ref. 59).

Western blotting. U2-OS cells were seeded in 10 cm^2 dishes. On the next day, the cells were synchronized by addition of 1 µM dexamethasone for 20 min. 23 h after synchronization, the cells were treated with either CORMs (dissolved in DMSO) or iCORMs (dissolved in ethanol) (100 µM final concentration, solvent was adjusted in all dishes) for 1 h. For harvesting, cells were washed with PBS, lysed in RIPA buffer (1× PBS, 1% IGEPAL CA-630, 0.5% Na-deoxycholate and 0.1% SDS) containing protease-inhibitor cocktail (Sigma-Aldrich). Lysates were homogenized by passage 5–10 times through a 21-gauge syringe needle and then centrifuged. The protein concentrations of the supernatants were determined with BCA assays. 25 µg of total protein was denatured in NuPAGE LDS loading buffer (Life Technologies) by boiling for 5 min at 95 °C, separated by SDS–PAGE with NuPAGE 4–12% Bis-Tris gels (Life Technologies) according to the manufacturer's protocol, transferred to a nitrocellulose membrane and incubated with an anti-BMAL1 primary antibody (gift from M. Brunner; validated in ref. 17) and anti-β-actin (A3853, Sigma-Aldrich). The next day, membranes were probed with HRP-conjugated secondary antibodies (sc-2317, Santa Cruz Biotechnologies), and a chemiluminescence assay was performed using Super Signal West Pico substrate (Pierce) followed by protein detection with a ChemoCam Imager (INTAS).

Determination of HO activity. HO activity was determined as previously described[60]. Briefly, lysates of cultured cells were prepared by mixture with lysis buffer (100 mM Tris/HCl, 150 mM NaCl and 1% Triton X-100, pH 7.4) and analyzed for the amount of total protein with Coomassie blue. The reactions were performed with 10 µl (20–100 µg total protein) of the crude lysates in 100 mM Tris-HCl with 15 µM hemin, 0.8 mM NADPH, 1 mM $MgCl_2$, 0.8 mM glucose-6-phosphate, 300 µM BSA and 1 U glucose-6-phosphate dehydrogenase and 3 µl of a bacterial lysate of biliverdinreductase (BVR)-overexpressing cells. The reaction samples were mixed, and 100 µl of the mixture was transferred into a black 96-well fluorescence microtiter plate (Nunc) in triplicates. Fluorescence emission was detected at a wavelength of 528 nm (±2 nm) in a fluorescence reader (Infinte M200, Tecan) at 37 °C with excitation at 441 nm, with a gain value of 140. Fluorescence was monitored every 3 min over 1.5 h and was detected five times per well and time point. The arithmetic mean was used to calculate the slope of the linear increase in fluorescence. HO activities were determined on the basis of an empirical value of 0.14 pmol bilirubin production per unit of fluorescence.

Chromatin immunoprecipitation (ChIP). ChIP from liver tissue from male wild-type (C57Bl/6) or *Bmal1*$^{-/-}$ mice (**Fig. 2f**) was performed as previously described[61]. Primers for the E-box-containing region in the mouse *Ho-1* promoter were: 5′-TGCAACAGCAGCGAGAAC-3′ (forward), 5′-GAAACTC TGGAGGCGACTG-3′ (reverse) and 5′-FAM-CCACCACGTGACCCGCGTAC-TAMRA-3′ (probe). As a positive control for BMAL1 binding, we used the upstream region of *Rev-Erbα* with 5′-TCACATGGTACCTGCTCCAG-3′ (forward), 5′-CTTTTGCCCGAGCCTTTC-3′ (reverse) and 5′-FAM-ACAGAG GGCTCTGCGCAGGC-TAMRA-3′ (probe); as a negative control, we used the promoter region of *Bmal1* with 5′-AGCGAGCCACGGTGAGTGT-3′ (forward), 5′-CCGGGAACTCGCGACCC-3′ (reverse) and 5′-FAM-AGCC GTCTCGGGGCGTCCCG-TAMRA-3′ (probe). For carbon monoxide treatment (**Fig. 4b**), U2-OS cells were grown in 15-cm dishes to 95% confluence. Cells were synchronized with 1 µM dexamethasone for 1 h and treated with either 100 µM CORMs or iCORMs for 1 h before cross-linking at the described time points. Cross-linking, chromatin preparation and chromatin immunoprecipitation were performed as described in ref. 61, with modifications. Cells were sonicated on ice for 15 s five times at a 50% setting, then centrifuged for 10 min (16,000*g*). Supernatants were diluted in buffer (1.1% Triton X-100, 2 mM EDTA, 150 mM NaCl and 20 mM Tris-HCl, pH 8.1) and incubated with anti-BMAL1 antibody[13] (a kind gift from M. Brunner), for 1 h under rotation (RT); agarose-A bead slurry in the same buffer was then added, and samples were incubated for 1 h under rotation (RT). Precipitates were washed sequentially in TSE I (0.1% SDS, 1% Triton X-100, 2 mM EDTA, 20 mM Tris-HCl, pH 8.1, and 150 mM NaCl), TSE II (0.1% SDS, 1% Triton X-100, 2 mM EDTA, 20 mM Tris-HCl, pH 8.1, and 500 mM NaCl), TSE III (0.25 M LiCl, 1% NP-40, 1% deoxycholate, 1 mM EDTA and 10 mM Tris-HCl, pH 8.1) and TSE IV (10 mM Tris-HCl, pH 8.1, 150 mM NaCl and 1 mM EDTA). Cross-linking was reversed at 65 °C in TSE V (20 mM Tris-HCl, pH 7.5, 150 mM NaCl, 2 mM EDTA and 1% SDS) overnight. DNA fragments were purified with a QIAquick Spin Kit (Qiagen) and eluted in 60 µl TE buffer. Q-PCR was performed with SYBR Green (Fermentas) on a CFX384 Real-Time PCR Detection System (Bio-Rad). For detection of BMAL1 binding to an E box in the promoter region of the human *Rev-erbα* gene, the primers (1 µM) 5′-CCTTCTCTGGACTTTGCCCT-3′ (forward) and 5′-AAACCTTGCAAACGTGAGGG-3′ (reverse) were used.

Real-time quantitative PCR. Total RNA was prepared with a PureLink RNA Mini Kit (Life Technologies) with an additional DNase treatment step (PureLink DNase (Life Technologies)) and then reverse transcribed to cDNA with RevertAid H Minus Reverse Transcriptase and 500 µM random pentadecamers (MWG). Quantitative PCR was performed with a CFX96 detection system (Bio-Rad) with Maxima SYBR Green master mix (Fermentas) and QuantiTect Primer Assays (Qiagen) and the following primers for mouse *Gapdh*, 5′-ACGGGAAGCTCACTGGCATGGCCTT-3′ (forward), 5′-CATGAG GTCCACCACCCTGTTGCTG-3′ (reverse). The primers for analysis of pre-mRNA were as follows: *Dbp*, 5′-GCTCTGAGAACGCAGACCTC-3′ (forward), 5′-AGGTCATTAGCACCTCCACG-3′ (reverse); *Rev-Erbα*, 5′-CCCTCCCCTTGTGTTCTCTT-3′ (forward), 5′-CTGCCATTGGAGCT GTCACT-3′ (reverse); *Bmal1*, 5′-TGTCGCACATCTGTATTGACG-3′ (forward), 5′-CTTCCATGAGGGTCATCTTTGT-3′ (reverse); *Pck1*, 5′-TTCTC TGGCCTGCAACTTTC-3′ (forward), 5′-TTGTCTTCACTGAGGTGCCA-3′ (reverse); *G6pc*, 5′-GGCTGATGCCTTGACAGTCT-3′ (forward), 5′-AG TATACACCTGCTGCGCCC-3′ (reverse); *Lpl*, 5′-TCATTTCACATAGATG CTTGCC-3′ (forward), 5′-GGGCACCCAACTCTCATACA-3′ (reverse); *Cyp7a1*, 5′-CCCCCATATGTCTCCTTCCA-3′ (forward), 5′-TAAATGGCAT TCCCTCCAGA-3′ (reverse). The transcript levels for each gene were normalized to those of *Gapdh* or *Hprt* and evaluated according to the $2^{-\Delta\Delta Ct}$ method[62].

Carbon monoxide gas treatment. Cells were cultured in sodium bicarbonate– and phenol red–free DMEM (Sigma-Aldrich) containing 10% FCS, 100 U/ml penicillin, 100 µg/ml streptomycin and 25 mM HEPES. For bioluminescence recordings (**Fig. 5c**), reporter cells were seeded in 35-mm dishes and incubated with 250 µM D-luciferin in light- and gas-tight aluminum boxes, including single photomultiplier tubes (Hamamatsu Photonics). For gene-expression studies (**Fig. 3b** and **Supplementary Fig. 2**) cells were seeded in 24-well plates and incubated in gas mixtures of 6% carbon monoxide (99.97%; Linde AG) with 94% air or 6% nitrogen (99.99%; Linde AG) with 94% air generated with DIGAMIX gas-mixing pumps (H. Wösthoff). These pumps have the highest accuracy for preparing high-quality calibration gas mixtures from pure gases. The gas mixtures were humidified to 100% and passed with a flow of 20–30 ml/min through gas-tight tubes, and aluminum or Plexiglas boxes incubated at 37 °C. According to Henry's law, 6% CO results in an ~50 µM CO concentration in aqueous solution at 37 °C (ref. 63).

Carbon monoxide–releasing molecules (CORMs). CORMs (tricarbonyldichl ororuthenium(II) dimer; $[Ru(CO)_3Cl_2]_2$) or iCORMs (ruthenium(III) chloride; $RuCl_3$) were purchased from Sigma-Aldrich and dissolved in a mixture of DMSO and ethanol. 1 mol CORMs dissociates into 4 mol CO. We used 400 µM CO in these experiments, a concentration eight times higher than 6% CO (50 µM); however, in contrast to that from constant gas treatment, CO from CORMs volatizes very rapidly, and only an undefined concentration reaches the cells.

Glucose production assay. 48 h after cell attachment, hepatocytes were synchronized with 1 µM dexamethasone (Dex) for 1 h, washed twice with PBS and incubated overnight with phenol red–free DMEM containing 5 mM glucose, 0.5% FBS and 100 nM glucagon. The next morning, cells were washed twice. Then the medium was replaced with phenol red–free and glucose-free medium supplemented with 2 mM pyruvate, 20 mM lactate and 100 nM glucagon for 5 h. The glucose concentration in the medium was determined with an Amplex Red Glucose Assay Kit (Invitrogen) according to the manufacturer's instructions. Total protein content was determined with the bicinchoninic acid (BCA) method (Thermo Scientific) for normalization.

Microarray experiments. Primary hepatocytes from *Ho-1*$^{-/-}$ 14- to 16-week-old male mice or their wild-type littermates with or without additional *Ho-2* depletion were synchronized with dexamethasone. 24 h after synchronization, total RNA was isolated with a PureLink RNA Mini Kit (Life Technologies) with an additional DNase treatment step (PureLink DNase (Life Technologies)). The integrity and amount of total RNA were analyzed with an Agilent 2100 Bioanalyzer. Synthesis of cDNA, amplification, labeling and hybridization were performed by the Labor für Funktionelle Genomforschung (LFGC) with GeneChip Mouse Gene 1.0 ST arrays (Affymetrix).

Bioinformatics analysis. All steps of the bioinformatics analysis were performed in R 2.15.0 (http://www.R-project.org/). Raw data from Affymetrix arrays were preprocessed and RMA normalized with the 'affy' package[64]. Differentially expressed probe sets were identified with an empirical Bayes approach implemented in the 'limma' package[65]. A minimum expression value of 6 on at least two arrays was set as a threshold. The false discovery rate was set to 0.05, and a minimum fold change of 1.5 was assumed between two experimental groups. Selected probe sets were clustered into six groups by application of a *k*-means algorithm to the scaled data. To ensure a robust reproducible solution, 100 random start sets for the cluster centers were used. Subsequently, probe sets were mapped to the associated genes. Identification of GO terms with an over-representation of associated genes in the clusters was performed with a classical Fisher test implemented in the package 'topGO' (version 2.10.0; http://www.bioconductor.org/packages/release/bioc/html/topGO.html). Because of the high redundancy of the GO hierarchy, no adjustment for multiple testing was done. Overlaps with data sets from Hughes *et al.*[16] and Rey *et al.*[17] were analyzed with the Fisher test with a multiple-testing Bonferroni correction of the *P* values. Circadian transcripts from Hughes *et al.*[16] were identified after fitting of the array data to a cosine-model with a Bonferroni-corrected *P* value <0.05, a minimal magnitude of six and a minimal amplitude of 0.5. E-box motifs from Rey *et al.*[17] were used to calculate the TRAP scores[66] genome wide for all promoter regions from −1,000 to 1,000 bp relative to the potential transcription start site[67]. The maximum number of background sets was randomly sampled without replacement in the same sizes as the foreground sets (genes in clusters), and the scores were tested for higher values in the foreground sets with single-sided Wilcoxon rank-sum tests. All *P* values were $\log_{10}$-transformed for plotting, and the geometric mean was calculated.

Statistics, sample size and conditions. Statistical test are described in the respective figure legends or in the section above. Sample sizes were not predetermined by statistical methods, and experiments were not randomized or conducted blind to conditions.

Data availability. The microarray data of this study have been deposited in the NCBI Gene Expression Omnibus (GEO) database and are accessible through GEO series accession number GSE55448. Source data for all other experiments are available on request.

49. Sandrelli, F. *et al.* A molecular basis for natural selection at the timeless locus in *Drosophila melanogaster*. *Science* **316**, 1898–1900 (2007).
50. Bischof, J., Maeda, R.K., Hediger, M., Karch, F. & Basler, K. An optimized transgenesis system for *Drosophila* using germ-line-specific phiC31 integrases. *Proc. Natl. Acad. Sci. USA* **104**, 3312–3317 (2007).
51. Renn, S.C., Park, J.H., Rosbash, M., Hall, J.C. & Taghert, P.H. A pdf neuropeptide gene mutation and ablation of PDF neurons each cause severe abnormalities of behavioral circadian rhythms in *Drosophila*. *Cell* **99**, 791–802 (1999).
52. Sepp, K.J., Schulte, J. & Auld, V.J. Peripheral glia direct axon guidance across the CNS/PNS transition zone. *Dev. Biol.* **238**, 47–63 (2001).
53. Dimitroff, B. *et al.* Diet and energy-sensing inputs affect TorC1-mediated axon misrouting but not TorC2-directed synapse growth in a *Drosophila* model of tuberous sclerosis. *PLoS One* **7**, e30722 (2012).
54. Chen, K.F., Peschel, N., Zavodska, R., Sehadova, H. & Stanewsky, R. QUASIMODO, a novel GPI-anchored zona pellucida protein involved in light input to the *Drosophila* circadian clock. *Curr. Biol.* **21**, 719–729 (2011).
55. Levine, J.D., Funes, P., Dowse, H.B. & Hall, J.C. Signal analysis of behavioral and molecular cycles. *BMC Neurosci.* **3**, 1–25 (2002).
56. Wilson, C.G. *et al.* Liver-specific overexpression of pancreatic-derived factor (PANDER) induces fasting hyperglycemia in mice. *Endocrinology* **151**, 5174–5184 (2010).
57. Gekakis, N. *et al.* Role of the CLOCK protein in the mammalian circadian mechanism. *Science* **280**, 1564–1569 (1998).
58. Maier, B. *et al.* A large-scale functional RNAi screen reveals a role for CK2 in the mammalian circadian clock. *Genes Dev.* **23**, 708–718 (2009).
59. Locke, J.C.W. *et al.* Extension of a genetic network model by iterative experimentation and mathematical analysis. *Mol. Syst. Biol.* **1**, 2005.0013 (2005).
60. Klemz, R., Mashreghi, M.F., Spies, C., Volk, H.D. & Kotsch, K. Amplifying the fluorescence of bilirubin enables the real-time detection of heme oxygenase activity. *Free Radic. Biol. Med.* **46**, 305–311 (2009).
61. Ripperger, J.A. & Schibler, U. Rhythmic CLOCK–BMAL1 binding to multiple E-box motifs drives circadian *Dbp* transcription and chromatin transitions. *Nat. Genet.* **38**, 369–374 (2006).
62. Livak, K.J. & Schmittgen, T.D. Analysis of relative gene expression data using real-time quantitative PCR and the $2^{-\Delta\Delta CT}$ method. *Methods* **25**, 402–408 (2001).
63. Lide, D.R. *CRC Handbook of Chemistry and Physics: a Ready-Reference Book of Chemical and Physical Data* (CRC Press, 1995).
64. Gautier, L., Cope, L., Bolstad, B.M. & Irizarry, R.A. affy: analysis of Affymetrix GeneChip data at the probe level. *Bioinformatics* **20**, 307–315 (2004).
65. Smyth, G.K. in *Bioinformatics and Computational Biology Solutions Using R and Bioconductor* (eds. Gentleman, R., Carey, V., Huber, W., Irizarry, R. & Dudoit, S.) 397–420 (Springer, 2005).
66. Roider, H.G., Kanhere, A., Manke, T. & Vingron, M. Predicting transcription factor affinities to DNA from a biophysical model. *Bioinformatics* **23**, 134–141 (2007).
67. Flicek, P. *et al.* Ensembl 2012. *Nucleic Acids Res.* **40**, D84–D90 (2012).